

The monopole-multipole energy of the lattices considered in the text can be shown to be simple multiples of  $W_L^{(2)}$ , viz.,

$$E_{40} = (7/12)W_4^{(2)} \quad \text{and} \quad E_{30} = (5/42)W_3^{(2)}.$$

Averaged radial coefficients of the lattice potential,  $\bar{A}_{LM}$ , can be used to determine an analytic expression

for the monopole-multipole energy per mole of substance,

$$E_{L0} = -N \sum_M [(2L+1)/8\pi] \alpha_L \bar{A}_{LM}^2.$$

Comparison with the results of the above perturbation method yields the  $\bar{A}_{LM}$ , from which the multipole-multipole interactions can be determined.

## Re-examination of the Lattice Dynamics of White Tin Using a Modified Axially Symmetric Model

R. E. DEWAMES AND G. W. LEHMAN

*North American Aviation Science Center, Canoga Park, California*

(Received 10 February 1964)

Experimental measurements of both the specific heat and the Debye-Waller factor for (white) Sn suggest the presence of low-lying phonon branches. In addition, recent experiments by Rowell *et al.* displayed structure in the Sn-Sn superconductors tunneling characteristic curve associated with very low-energy Van Hove singularities in the Sn vibrational spectrum. A previous theoretical calculation of the Sn phonon spectrum using the elastic constants of Mason and Bömmel does not predict the existence of such low-lying phonon branches. A subsequent calculation based on the elastic data of Rayne and Chandrasekhar, on the other hand, clearly indicates the presence of a very low-energy acoustic branch along the [110] direction. However, in this calculation complete elastic consistency was not possible because of the constraint imposed by the *A-S* (axially symmetric) lattice dynamics model. Consequently, we have re-examined the lattice vibrational spectrum of Sn on the basis of a generalized *A-S* lattice dynamics model which allows complete elastic consistency to be obtained. The specific heat, the magnitude of the Debye-Waller factor and the low-energy structure in the tunneling experiments calculated from the dispersion curves obtained from our modified *A-S* model are in quantitative agreement with experimental observations. The anisotropy factor  $\epsilon$  of the Debye-Waller factor is increased from 1.2 to 1.56 and remains in disagreement with experiment. It appears to us that with the present elastic data it is not possible to obtain a mean-square displacement larger in the  $z$  direction than that in the  $x$  direction. Furthermore, we conclude that the Mason and Bömmel elastic data are incapable of explaining the present experimental data on white tin.

### I. INTRODUCTION

**E**XPERIMENTAL measurements of both the specific heat<sup>1</sup> and the Debye-Waller<sup>2-5</sup> factor for white tin suggest the presence of low-lying phonon branches. In addition, recent experiments by Rowell *et al.*<sup>6</sup> displayed structure in the Sn-Sn superconducting tunneling characteristic curve associated with very low-energy Van Hove singularities in the Sn vibrational spectrum.

A previous<sup>7</sup> theoretical calculation of the Sn phonon

spectrum using the axially symmetric lattice dynamics model (*A-S* model) with the elastic data of Mason and Bömmel<sup>8</sup> does not predict the existence of such low-lying phonon branches. A subsequent calculation,<sup>9</sup> based on the elastic data of Rayne and Chandrasekhar,<sup>10</sup> on the other hand, clearly indicated the presence of a very low-energy acoustic branch along the [110] direction. However, in this calculation complete elastic consistency was not possible because of the constraint imposed by the *A-S* model ( $C_{44} - C_{13} - C_{66} + C_{12} = 0$ ). Consequently, we have re-examined the lattice vibrational spectrum of Sn on the basis of a generalized *A-S* lattice dynamics model which allows complete elastic consistency to be obtained. This generalized *A-S* model will be described in more detail in a subsequent paper on the lattice vibrational spectrum of hexagonal close packed metals. Briefly the model allows the bond-

<sup>1</sup> R. Hultgren, R. L. Orr, P. D. Anderson, and K. K. Kelley, *Selected Values of Thermodynamic Properties of Metals and Alloys* (John Wiley & Sons, Inc., New York, 1963).

<sup>2</sup> W. H. Wiedemann, P. Kienle, and F. Pobell, *Z. Physik* **166**, 109 (1962).

<sup>3</sup> A. J. F. Boyle, D. St. P. Bunbury, C. Edwards, and H. E. Hall, *Proc. Phys. Soc. (London)* **A77**, 129 (1961).

<sup>4</sup> R. Barloutand, J. O. Picon, and C. Tzara, *Compt. Rend.* **250**, 2705 (1960).

<sup>5</sup> N. E. Alekseyevsky, Pham Zuy Hien, V. G. Shapiro, and V. S. Shunel, *Zh. Eksperim. i Teor. Fiz.* **43**, 790 (1962) [English transl.: *Soviet Phys.—JETP* **16**, 559 (1963)].

<sup>6</sup> J. M. Rowell, P. W. Anderson, and D. E. Thomas, *Phys. Rev. Letters* **10**, 334 (1963).

<sup>7</sup> T. Wolfram, G. W. Lehman, and R. E. DeWames, *Phys. Rev.* **129**, 2483 (1963).

<sup>8</sup> W. P. Mason and H. E. Bömmel, *J. Acoust. Soc. Am.* **28**, 930 (1956).

<sup>9</sup> R. E. DeWames, T. Wolfram, and G. W. Lehman, *Phys. Rev.* **131**, 529 (1963).

<sup>10</sup> J. A. Rayne and B. S. Chandrasekhar, *Phys. Rev.* **120**, 1658 (1960).

TABLE I. Elastic constants for white tin (in units of  $10^{11}$  dyne  $\text{cm}^{-2}$ ).

| Constant | Mason and Bömmel | Temperature                      |                                |
|----------|------------------|----------------------------------|--------------------------------|
|          |                  | 300°K<br>Rayne and Chandrasekhar | 4°K<br>Rayne and Chandrasekhar |
| $C_{11}$ | 7.33             | 7.23                             | 8.274                          |
| $C_{33}$ | 8.74             | 8.840                            | 10.31                          |
| $C_{44}$ | 2.19             | 2.203                            | 2.695                          |
| $C_{66}$ | 2.25             | 2.400                            | 2.818                          |
| $C_{12}$ | 2.38             | 5.94                             | 5.785                          |
| $C_{13}$ | 2.48             | 3.58                             | 3.421                          |

bending constant in the  $x$  direction to be different from that in the  $z$  direction, their ratio being defined by  $\sigma_B$ , an anisotropy factor.  $\sigma_B$  is uniquely determined from the elastic constants by the relation  $\sigma_B = (C_{44} - C_{12}) / (C_{66} - C_{12})$  provided  $C_{66} \neq C_{12}$ .

The results of the calculation are given in Sec. II, where we discuss the calculated vibrational spectrum, the Debye-Waller factor and the specific heat using the

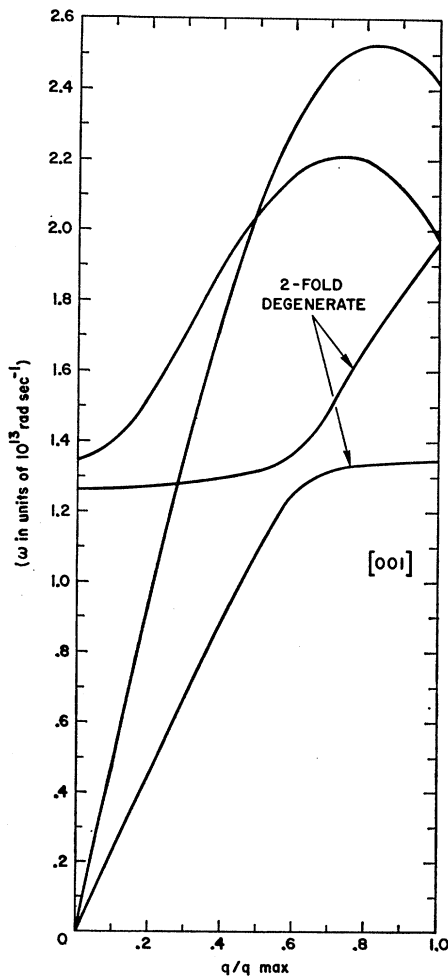


FIG. 1. Dispersion curves along the [001] direction for white tin using Rayne and Chandrasekhar's elastic data at 4°K.

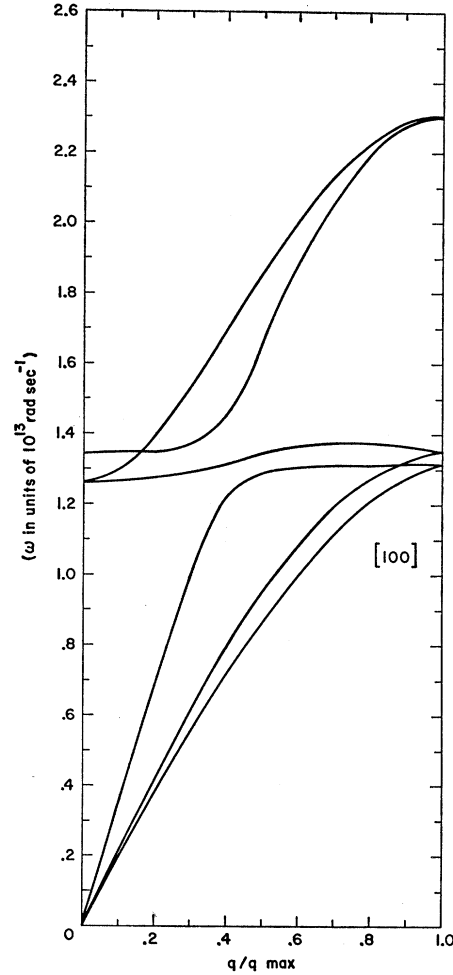


FIG. 2. Dispersion curves along the [100] direction for white tin using Rayne and Chandrasekhar's elastic data at 4°K.

elastic data of Rayne and Chandrasekhar at 4°K and at 300°K. For comparison, calculations are also made using Mason and Bömmel's elastic data without the additional constraint that the optical frequency at  $q=0$  be the Debye frequency.<sup>7</sup>

## II. DISCUSSION AND RESULTS

Table I gives the elastic data from which it is clear that the main difference between the results of both investigators is  $C_{12}$ . Table II gives the anisotropy factor  $\sigma_B$  for the elastic data of Rayne and Chandrasekhar. One does not need to introduce  $\sigma_B$  for the Mason and

TABLE II. Elastic anisotropy factor,  $\sigma_B$ .

| $\sigma_B$ | Temperatures |        |
|------------|--------------|--------|
|            | 300°K        | 4°K    |
|            | 0.3897       | 0.2447 |

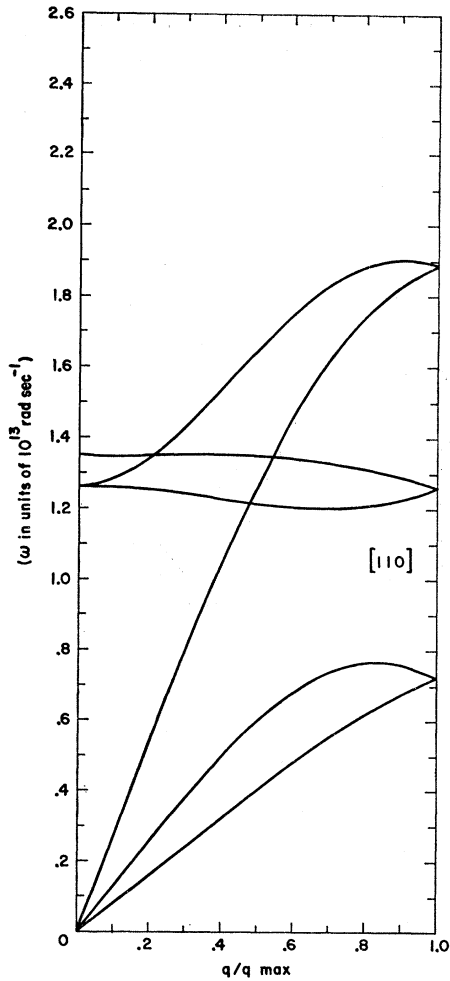


FIG. 3. Dispersion curves along the  $[110]$  direction for white tin using Rayne and Chandrasekhar's elastic data at  $4^\circ\text{K}$ .

TABLE III. Modified  $A$ - $S$  force constants (in units of  $10^4$  dyne  $\text{cm}^{-1}$ ).

| Constant    | Temperature      |                                  |                                |
|-------------|------------------|----------------------------------|--------------------------------|
|             | Mason and Bömmel | 300°K<br>Rayne and Chandrasekhar | 4°K<br>Rayne and Chandrasekhar |
| $K_1(1,12)$ | 1.082            | 0.914                            | 1.081                          |
| $C_2(1,12)$ | 0.0              | -0.451                           | -0.435                         |
| $K_1(2,11)$ | 1.805            | 1.802                            | 2.106                          |
| $C_2(2,11)$ | 0.0              | 0.0                              | 0.0                            |
| $K_1(3,12)$ | 1.017            | 1.143                            | 1.216                          |
| $C_2(3,12)$ | 0.0              | -0.112                           | -0.0368                        |
| $K_1(4,11)$ | 0.411            | 0.762                            | 0.786                          |
| $C_2(4,11)$ | 0.0              | 0.0                              | 0.0                            |

Bömmel elastic data. Table III gives the  $A$ - $S$  atomic force constants. The difference in the elastic data is reflected in the value of  $K(4,11)$  and the bond-bending constants. Arbitrarily setting  $C_2(2,11)$  and  $C_2(4,11)$  equal to zero, it is possible to satisfy all elastic equations, and hence to predict the vibrational spectrum entirely

from the elastic properties. In the calculation of the  $A$ - $S$  atomic force constants from the elastic constant we neglected the optical correction. Hence the slopes of the resulting dispersion curves for small  $q$  are lower than would be calculated from the elastic data.

Figures 1-3 give the vibrational spectrum along the principal directions using the elastic data of Rayne and Chandrasekhar at  $4^\circ\text{K}$ . The optical branches are considerably different from those previously obtained using the unmodified  $A$ - $S$  model.

Figures 4-6 give the dispersion curve using Rayne and Chandrasekhar's elastic data at  $300^\circ\text{K}$ . Comparison with the  $4^\circ\text{K}$  results shows that the vibrational spectrum is in general depressed. Note, in particular, the depression in the lower transverse branch along the  $[110]$  direction.

Figures 7-9 give the vibrational spectrum using Mason and Bömmel's elastic data. Clearly, one does not get the low-lying phonon branches needed to explain the observed properties of white tin.

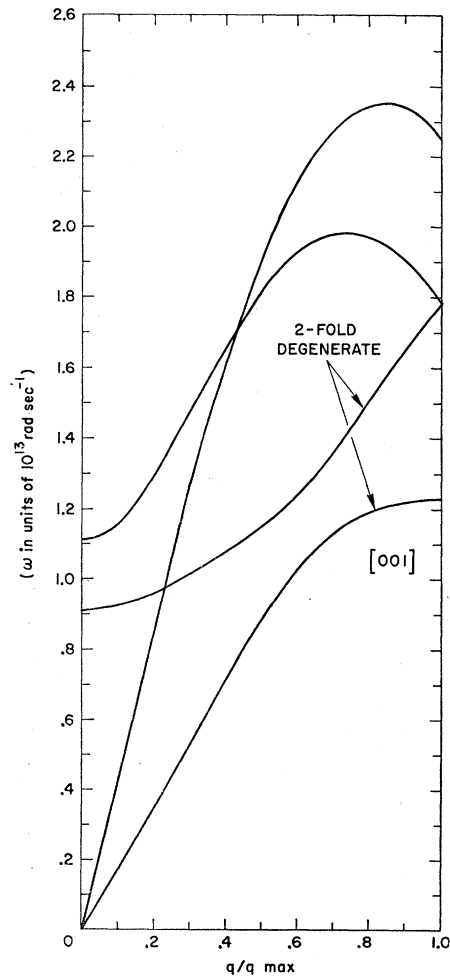


FIG. 4. Dispersion curves along the  $[001]$  direction for white tin using Rayne and Chandrasekhar's elastic data at  $300^\circ\text{K}$ .

TABLE IV. Comparison of experimental and calculated values for the total specific heat of white tin (in units of cal mole<sup>-1</sup> deg<sup>-1</sup>).

| T°K    | C <sub>p</sub> (exp) <sup>a</sup> | Rayne and Chandrasekhar elastic data, 4°K<br>C <sub>v</sub> (lattice) | Rayne and Chandrasekhar elastic data, 300°K<br>C <sub>v</sub> (lattice) | Mason and Bömmel elastic data 300°K<br>C <sub>v</sub> (lattice) |
|--------|-----------------------------------|---|---|---|
| 10     | 0.234                             | 0.092   | 0.18  | 0.079   |
| 15     | 0.618                             | 0.38  | 0.61  | 0.34  |
| 20     | 1.11                              | 0.887   | 1.23  | 0.82  |
| 25     | 1.65                              | 1.49  | 1.90  | 1.41  |
| 50     | 3.68                              | 3.84  | 4.16  | 3.81  |
| 75     | 4.74                              | 4.85  | 5.04  | 4.85  |
| 100    | 5.32                              | 5.31  | 5.43  | 5.31  |
| 125    | 5.65                              | 5.54  | 5.62  | 5.54  |
| 150    | 5.86                              | 5.68  | 5.73  | 5.68  |
| 200    | 6.10                              | 5.82  | 5.85  | 5.82  |
| 250    | 6.26                              | 5.88  | 5.90  | 5.88  |
| 286.2  | 6.40                              | 5.91  | 5.92  | 5.91  |
| 298.15 | 6.45                              | 5.92  | 5.93  | 5.92  |

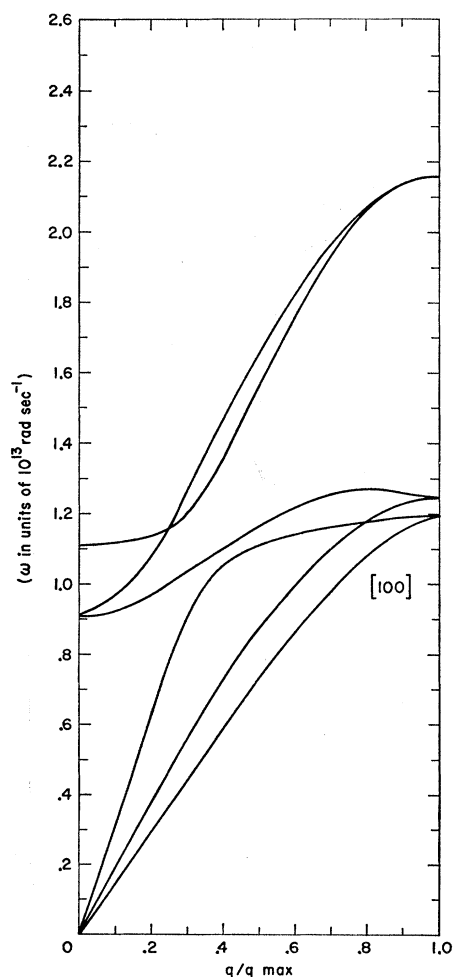
<sup>a</sup> See Ref. 1.

FIG. 5. Dispersion curves along the [100] direction for white tin using Rayne and Chandrasekhar's elastic data at 300°K.

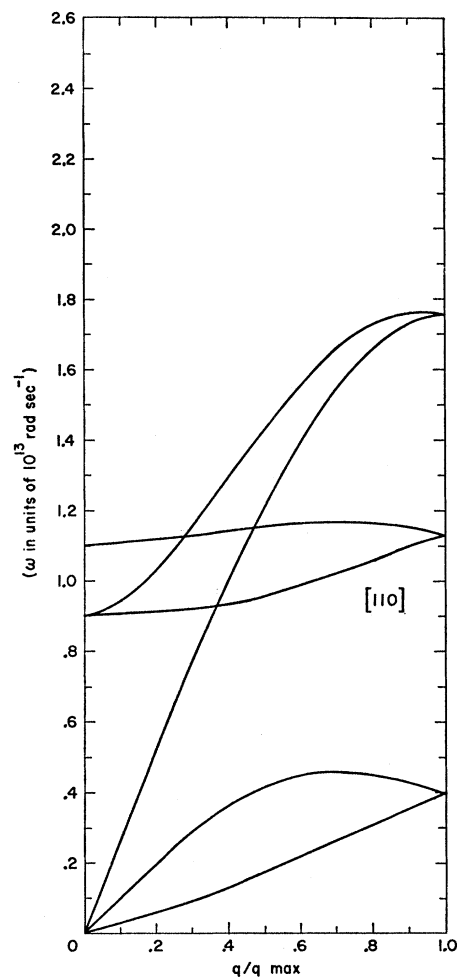


FIG. 6. Dispersion curves along the [110] direction for white tin using Rayne and Chandrasekhar's elastic data at 300°K.

The low-energy structure, observed by Rowell *et al.*<sup>6</sup> between 1.5 and 3.5 mV can be associated with the stationary points in  $\omega$  versus  $q$  in the low-lying phonon branches along the [110] direction which are predicted by the Rayne and Chandrasekhar elastic data.

Now, we turn our attention to Table IV where we have tabulated the predicted and experimental specific heat. Our values using Rayne and Chandrasekhar's elastic data at 300°K are still low and actually one needs an increase in the density of states around 10–15°K which corresponds in energy to the first discontinuity observed in the tunneling experiment.

In Fig. 10,<sup>11</sup>  $2W_x$  obtained from the values of  $H_{xx}$  in

<sup>11</sup> Our values of  $H_{xx}(T)$  defined in Ref. 9 should be divided by two. Consequently the Debye-Waller factor should be increased. This error came about because of a normalization of the polarization vectors in our program. Furthermore, Eq. (3) should read

$$g[\omega(q,j)] = \frac{1}{N_a \hbar \omega(q,j)} \left\{ \frac{2}{\exp[\hbar \omega(q,j)/kT] - 1} + 1 \right\},$$

where  $N_a$  is the total number of atoms.

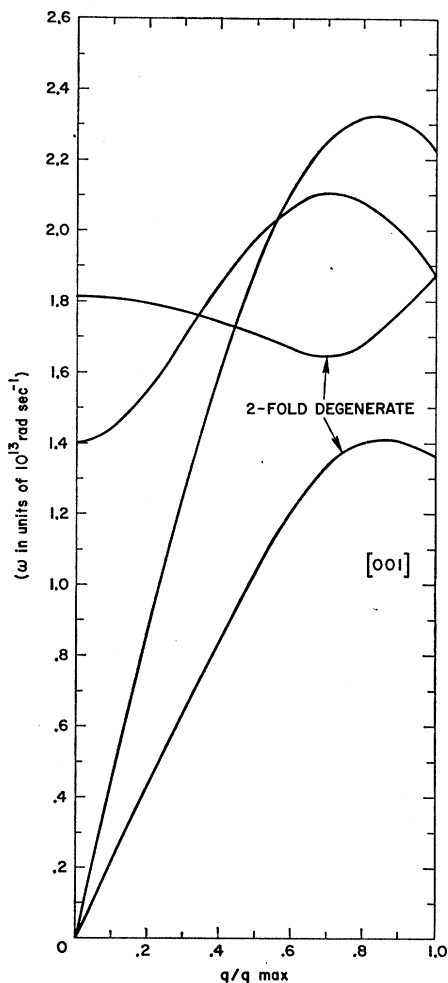


FIG. 7. Dispersion curves along the [001] direction for white tin using Mason and Bömmel's elastic data.

TABLE V. Temperature dependence of  $H_{zz}(T)$  and  $\epsilon(T)$ .

| $T^\circ\text{K}$ | Rayne and Chandrasekhar elastic data, $4^\circ\text{K}$ |               | Rayne and Chandrasekhar elastic data, $300^\circ\text{K}$ |               | Mason and Bömmel elastic data, $300^\circ\text{K}$ |               |
|-------------------|---|---------------|---|---------------|--|---------------|
|                   | $H_{zz}(T)$<br>(in units of $10^8\text{eV}^{-1}$ )      | $\epsilon(T)$ | $H_{zz}(T)$<br>(in units of $10^8\text{eV}^{-1}$ )        | $\epsilon(T)$ | $H_{zz}(T)$<br>(in units of $10^8\text{eV}^{-1}$ ) | $\epsilon(T)$ |
| 10                | 0.10  | 1.22          | 0.11  | 1.28          | 0.10   | 1.09          |
| 15                | 0.10  | 1.23          | 0.11  | 1.29          | 0.10   | 1.09          |
| 20                | 0.10  | 1.24          | 0.12  | 1.32          | 0.11   | 1.09          |
| 25                | 0.11  | 1.25          | 0.13  | 1.35          | 0.11   | 1.09          |
| 50                | 0.13  | 1.32          | 0.17  | 1.46          | 0.14   | 1.10          |
| 75                | 0.17  | 1.36          | 0.23  | 1.51          | 0.19   | 1.12          |
| 100               | 0.22  | 1.38          | 0.29  | 1.53          | 0.24   | 1.12          |
| 125               | 0.27  | 1.39          | 0.36  | 1.54          | 0.29   | 1.13          |
| 150               | 0.31  | 1.39          | 0.42  | 1.55          | 0.34   | 1.13          |
| 200               | 0.41  | 1.40          | 0.56  | 1.55          | 0.45   | 1.13          |
| 250               | 0.51  | 1.41          | 0.69  | 1.46          | 0.56   | 1.13          |
| 286.2             | 0.58  | 1.41          | 0.79  | 1.56          | 0.64   | 1.13          |
| 298.15            | 0.60  | 1.41          | 0.82  | 1.56          | 0.66   | 1.13          |
| 500               | 1.0   | 1.41          | 1.38  | 1.56          | 1.10   | 1.13          |

Table V is given. The values obtained from the vibrational spectrum of Rayne and Chandrasekhar's elastic data at  $300^\circ\text{K}$  gave the best fit to  $2W$ . Note that comparison is made with  $2W$  (polycrystal); hence, actually our full line should be lower somewhat since one needs to average the Debye-Waller factor  $e^{-2W}$  over all directions. In Table V, the anisotropy  $\epsilon$  in the mean-square displacement is tabulated. The mean-square displacement in the  $x$ - $y$  plane is still larger than that in the  $z$  plane in apparent contradiction with the conclusion of Alekseyevsky *et al.*<sup>5</sup> and Meechan *et al.*<sup>12</sup> from Mössbauer experiments. During our calculations we were able to demonstrate that the anisotropy  $\epsilon$  in the mean-square displacement is roughly governed by the elastic constant  $C_{33}$  and  $C_{11}$ . This can be easily understood since  $2W \propto 1/\omega^2$ . In fact, we interchanged the values of  $C_{33}$  and  $C_{11}$  and correspondingly obtained a reverse in the anisotropy factor  $\epsilon$ .

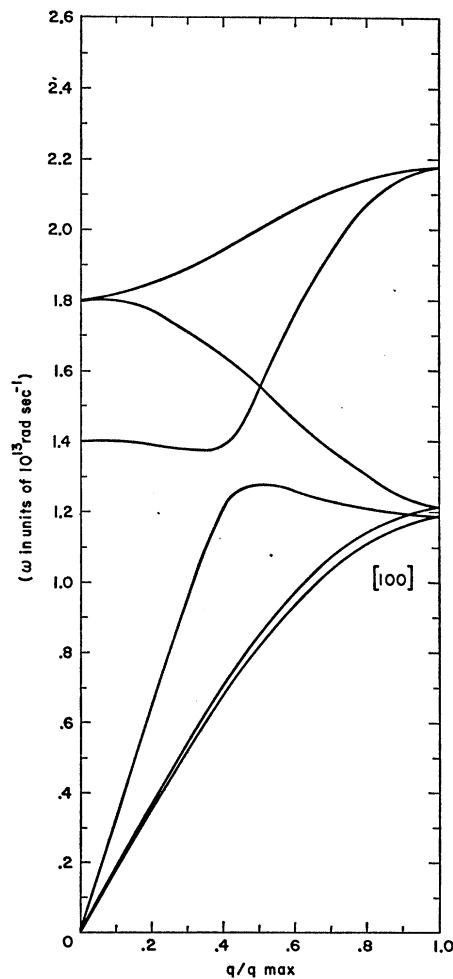


FIG. 8. Dispersion curves along the [100] direction for white tin using Mason and Bömmel's elastic data.

<sup>12</sup> C. J. Meechan, A. H. Muir, U. Gonser, and H. Wiedersich, *Bull. Am. Phys. Soc.* **7**, 600 (1962).

## III. CONCLUSION

In this paper we recalculated the vibrational spectrum of white tin using a modified  $A$ - $S$  model. Elastic consistency is obtained by introducing an anisotropy parameter  $\sigma_B$  which essentially allows the bond bending in the  $z$  direction to be different than that in the  $x$  direction. We have shown that in order to explain the low-lying phonons observed in the tunneling experiment, the low values of the Debye-Waller factor and the large values of the specific heat at low temperatures one needs the elastic data of Rayne and Chandrasekhar which give large values for  $C_{12}$  rather than those of Mason and Bömmel.

In the following let us make a few conjectures. The properties of white tin suggest the need for even lower lying phonon branches than those obtained using the

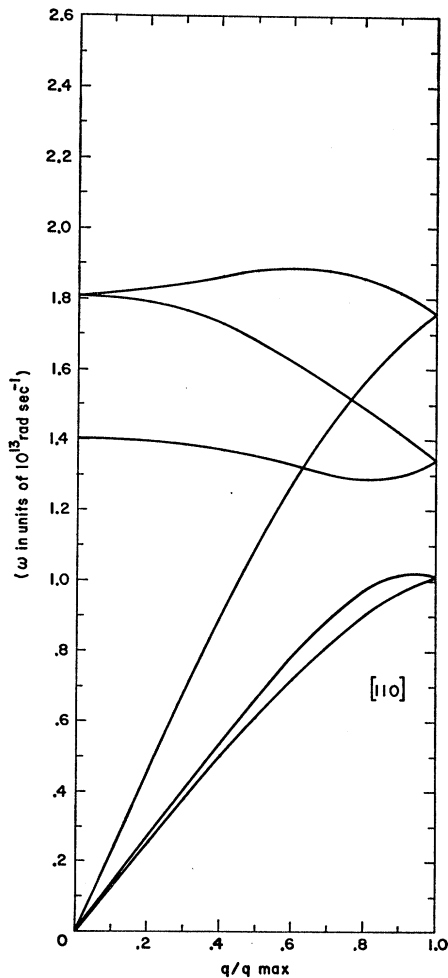


Fig. 9. Dispersion curves along the  $[110]$  direction for white tin using Mason and Bömmel's elastic data.

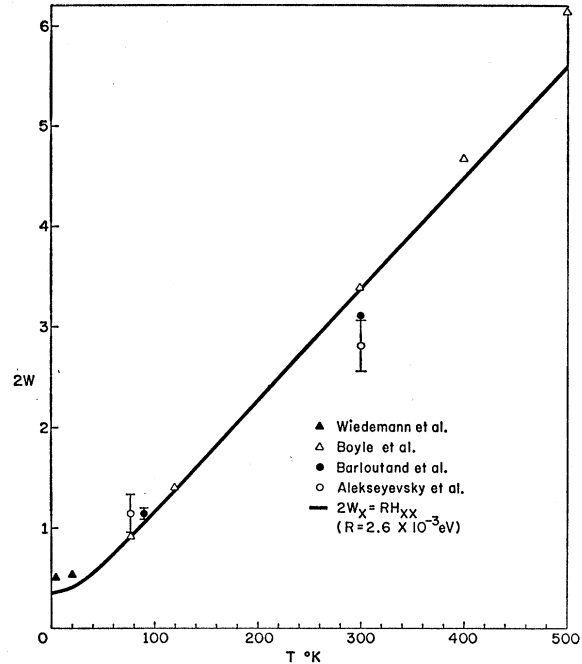


Fig. 10. Comparison of experimental and calculated values of  $2W$ .

modified  $A$ - $S$  model. We feel that the lower transverse branch along the  $[110]$  direction given by the Rayne and Chandrasekhar elastic data should show more dispersion at higher  $q$  than predicted by the modified  $A$ - $S$  model. This could easily be accounted for by the effect of more distant neighbors not included in the lattice dynamics model. If this is the case, because the upper transverse branch must be equal to the lower transverse branch at  $q=q_{\max}$  along  $[110]$  direction one could obtain two increases in the density of states closely spaced in frequency. The first arising because of the flattening of the lower transverse branch, the second because the upper transverse branch must change slope in order to equal the lower branch at  $q_{\max}$ . It is possible that the low-energy singularities observed by Rowell *et al.*<sup>6</sup> arise from portions of the Brillouin zone other than points of high symmetry. In order to discuss quantitatively the results of Rowell *et al.*<sup>6</sup> the density of states is required.

## ACKNOWLEDGMENTS

We wish to acknowledge several stimulating discussions on the subject matter of this paper with Dr. T. Wolfram. We are also indebted to Dr. J. M. Rowell for communicating to us his experimental superconducting tunneling data on Sn.